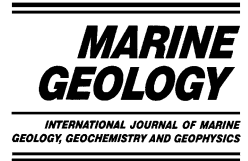




ELSEVIER

Marine Geology 186 (2002) 487–504



www.elsevier.com/locate/margeo

# Paleoproductivity in the southern Peru–Chile Current through the last 33 000 yr

Dierk Hebbeln<sup>a,\*</sup>, Margarita Marchant<sup>b</sup>, Gerold Wefer<sup>a</sup>

<sup>a</sup> *Geowissenschaften, Universität Bremen, P.O. Box 330440, D-28334 Bremen, Germany*

<sup>b</sup> *Departamento Zoología, Facultad Ciencias Naturales y Oceanográficas, Universidad de Concepción, Casilla 160-C, Concepción, Chile*

Received 20 September 2001; accepted 18 April 2002

## Abstract

Based on a multiparameter approach including organic carbon, biogenic opal, carbonate and the species composition of planktic foraminifera, this paper provides the first qualitative assessment of the history of paleoproductivity on glacial–interglacial time scales in the southern Peru–Chile Current (PCC) off Chile, which belongs to the least studied parts of the world ocean. During the Last Glacial Maximum (LGM) highest relative paleoproductivity of the last 33 kyr, indicated by high accumulation rates of organic carbon, biogenic opal and carbonate, has been found, contrasted by lowest values during the early and Middle Holocene. This shift from high to low productivity is accompanied by a major change in the species composition of planktic foraminifera from a dominance of *Neogloboquadrina pachyderma* (sin.) to the dominance of *N. pachyderma* (dex.). The temporal pattern of paleoproductivity off Chile is very similar to the history of the continental paleoclimate in the region, which is supposed to be driven by the position of the Southern Westerlies. This observation points to a functional relationship between the position of the Southern Westerlies and the history of paleoproductivity off Chile. Assuming that atmospheric and oceanographic circulation are closely linked, a northward displacement of the Antarctic Circumpolar Current during the LGM, in line with the northward movement of the Southern Westerlies, would bring the main nutrient source closer to our core sites resulting in increased productivity. However, based on the available data, it is not clear if the higher productivity in the southern PCC during the LGM reflects generally higher productivity during this time or only a regional displacement of the main productivity centers. © 2002 Elsevier Science B.V. All rights reserved.

**Keywords:** SE Pacific; Peru–Chile Current; paleoproductivity; planktic foraminifera

## 1. Introduction

The pattern of changing atmospheric contents of the major greenhouse gas carbon dioxide be-

tween low glacial and high interglacial values, which runs parallel to cold and warm periods of the Earth's climate in the Late Quaternary (Barnola et al., 1987), is assumed to at least partly result from variations in the productivity of the oceans (Broecker, 1982). Increased productivity by marine algae results in an increased drawdown of atmospheric carbon dioxide into the ocean by photosynthetic fixation in organic matter and the

\* Corresponding author. Tel.: +49-421-2189079; Fax: +49-421-2188916.

E-mail address: dhebbeln@uni-bremen.de (D. Hebbeln).

subsequent deposition of parts of it in the ocean sediments (Berger et al., 1989). However, marine productivity is rather uneven distributed over the world ocean, as ~50% of it takes place on only 15% of the world ocean area (Berger et al., 1989), namely in the high productivity regions associated with the equatorial and subpolar divergence zones and the eastern boundary currents. Thus, major changes in the paleoproductivity of the world ocean, able to significantly affect the atmospheric carbon dioxide content, are most likely related to these high productivity regions.

For some of these areas assessments of the paleoproductivity on glacial–interglacial time scales exist, although the conclusions drawn are not always unequivocal. For some equatorial and coastal upwelling areas the available data point to higher productivity during glacials (Berger and Herguera, 1992; Lyle, 1988; McIntyre et al., 1989; Rühlemann et al., 1999; Sarnthein and Winn, 1990; Schneider et al., 1996). From the Antarctic increased (Keir, 1990) as well as decreased (Mortlock et al., 1991) glacial productivities have been reported. These observations are now interpreted to reflect merely a latitudinal shift of the high productivity zone rather than significant quantitative changes in productivity (Mackensen et al., 1994).

Among the eastern boundary currents the Peru–Chile Current (PCC) stands out with an extension over 40° of latitude. With its persistent coastal upwelling it belongs to the most productive marine environments (Berger et al., 1987) supporting an intensive pelagic fishery (Alheit and Bernal, 1993). However, about its southern part extending over 20° of latitude along the Chilean coast, only little information based on marine sediments is available focusing mostly on terrigenous sediments (Lamy et al., 1998, 1999, 2000). Only one analysis of planktic foraminifera covering the last 13 kyr reveals some information about the paleoproductivity of the region (Marchant et al., 1999). Here we provide the first estimate of paleoproductivity variations in the southern PCC on glacial–interglacial time scales based on a multiparameter approach using accumulation rates of various biogenic sediment components and the species composition of planktic foraminifera.

## 2. Regional setting

The regional oceanography of the Southeast Pacific has recently been described by Shaffer et al. (1995) and by Strub et al. (1998). The circulation pattern is dominated by the northward flowing PCC (Subantarctic Surface Water; Fig. 1), which originates between 40 and 45°S where the Antarctic Circumpolar Current (ACC) approaches the South American continent (Boltovskoy, 1976). The northward deflection of the ACC mainly forms the PCC, which stretches all along the South American west coast before it turns westward close to the equator to form the South Equatorial Current.

Off the Chilean coast occasionally the PCC can be divided into an oceanic (PCCocean) and a coastal (PCCcoast) branch separated by the poleward flowing Peru–Chile Countercurrent (PCCC, Subtropical Surface Water) (Fig. 1). The coastal branch of the PCC is also termed Chilean Coastal Current and is characterized by a significant admixture of low salinity surface waters derived from the Chilean fjord region. It extends to ~100 km off the coast followed by the PCCC, 100–300 km offshore, while further to the west the oceanic branch of the PCC prevails. Close to the coast these surface water masses are underlain by the poleward flowing Gunther Undercurrent (Equatorial Subsurface Water), which is mainly located between 100 and 400 m water depth over the shelf and the continental slope. Between 400 and 1200 m water depth Antarctic Intermediate Water flows equatorwards underlain by sluggishly southward flowing Pacific Deep Water.

Perennial southerly winds result in Ekman drift-induced upwelling of cool, nutrient-rich waters along the Chilean coast (Brandhorst, 1963). Due to the continuous and intense coastal upwelling the PCC belongs to the most important high productivity regions in the world ocean (Berger et al., 1987). Although the winds are upwelling-favorable throughout the year (Strub et al., 1998) the physical and the biological settings display distinct seasonal patterns. Off Valparaiso primary productivity is highest during the austral winter (Thomas et al., 1994) when sea surface temperatures are lowest. During this time the

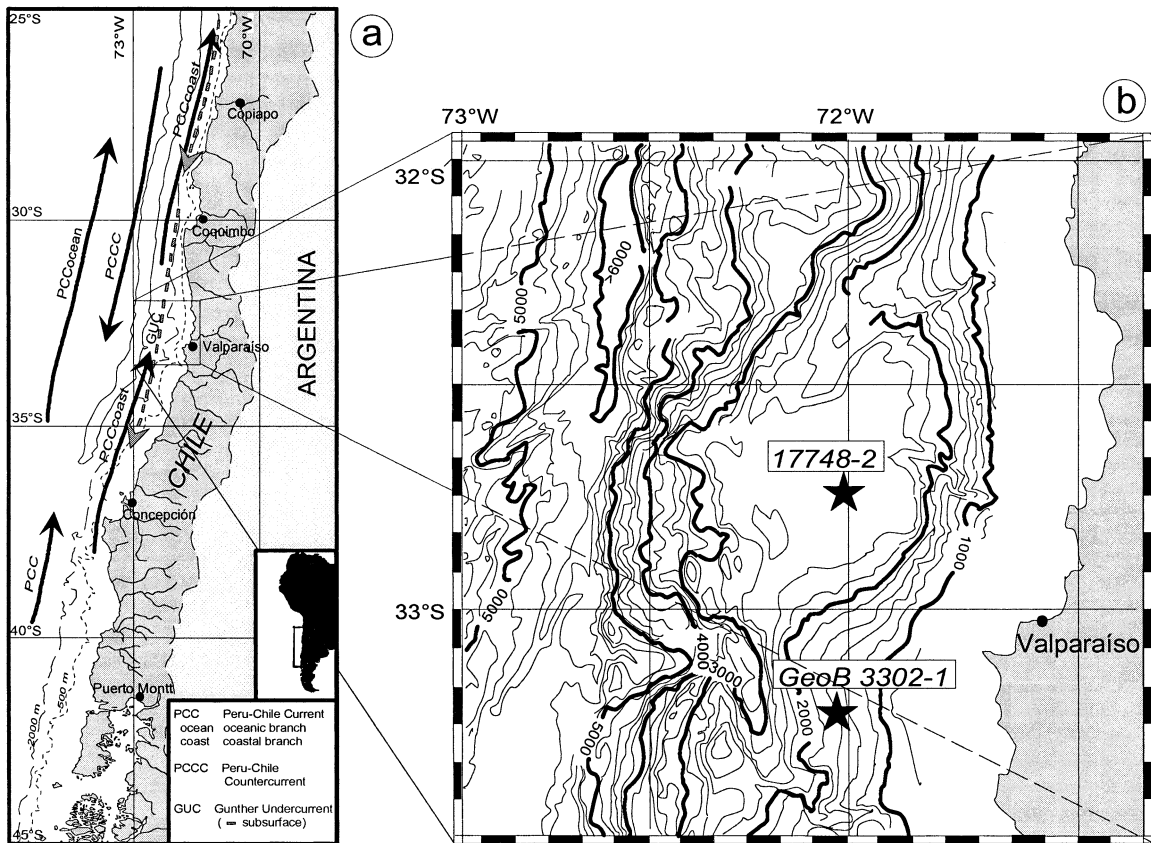


Fig. 1. (a) Oceanographic setting along the Chilean continental slope according to Strub et al. (1998). (b) Morphological setting of the two core sites at the Chilean continental slope off Valparaíso.

wind direction shifts from predominantly southeasterly to southwesterly directions. The particle flux in the PCC reflects this seasonal pattern with highest fluxes in late winter (September), intermediate fluxes until January and low fluxes between January and July (Hebbeln et al., 2000b). Investigation of surface sediments from the Chilean continental slope points to the ACC as the principal nutrient source that sustains the high productivity in the southern PCC, where, besides being slowly consumed, the nutrients are continuously recycled in the coastal upwelling system while moving to the north (Hebbeln et al., 2000a).

The two sediment cores investigated here have been retrieved from the Chilean continental slope close to Valparaíso off central Chile at approximately 33°S (Fig. 1). Core 17748-2 (32°45.0'S, 72°02.0'W, water depth 2545 m, length 383 cm)

was retrieved during cruise SONNE-80 (Stoffers and Shipboard Scientific Party, 1992) from the southern part of the Valparaíso Basin, which is a 50 by 50-km-wide, flat area at water depths between 2400 and 2600 m on the continental slope (Fig. 1). A small transverse ridge divides the basin in a northern and a southern part. The upper slope rises steeply towards the coast and is cut by two large canyons, which both end in the northern part of the basin. Core GeoB 3302-1 (33°13.1'S, 72°05.4'W, water depth 1498 m, length 412 cm) was retrieved during cruise SONNE-102 (Hebbeln et al., 1995) approximately 50 km further south on the moderately inclined (~3°) upper continental slope (Fig. 1). This location is about 20 km north of the San Antonio canyon, a major submarine canyon off the mouth of the Maipo River.

### 3. Methods

The two gravity cores were sampled at 5-cm intervals. One sample set was ground for geochemical analyses, while another sample set was washed over a 63- $\mu\text{m}$  sieve to separate the coarse fraction for foraminifera analyses. The dry bulk density of the sediments was measured by weighing a fixed sample volume before and after freeze-drying.

#### 3.1. Geochemical analyses

To analyze the total organic carbon (TOC) content 25 mg of the sample material has been decalcified with 6 N HCl, dried on a hot plate at 80°C and measured in a Heraeus-CHN elementary analyzer. Carbonate contents were calculated from the total carbon (TC) content, measured with the CHN analyzer on untreated samples, as:

$$\text{CaCO}_3 = \text{TC} - \text{TOC} * 8.333 \quad (1)$$

with a standard deviation of <2% of the measured value for TOC as well as for TC measurements.

Biogenic opal was determined using a sequential leaching technique (DeMaster, 1981) modified by Müller and Schneider (1993). The ground samples were extracted with 100 ml 1 M NaOH at 85°C. The concentration of dissolved silica was simultaneously measured by continuous flow analysis with molybdate blue spectrometry. The standard deviation for sediments with biogenic opal contents <5%, as it is the case here, is given with 10% of the measured value (Müller and Schneider, 1993). The biogenic opal content has been measured only in 10-cm intervals (and in 20-cm intervals in the lowermost part of core 17748-2 with sediments older than 13 000 yr).

#### 3.2. Foraminifera analyses

The analyses of the planktic foraminiferal fauna are based on the >150- $\mu\text{m}$  fraction, which was separated by sieving from the >63- $\mu\text{m}$  fraction. Using a microsplitter the samples were divided to a sample size of approximately 200 indi-

viduals. All specimens were individually picked and identified using the planktic foraminifera taxonomy of Parker (1962), Kennett and Srinivasan (1983), and Hemleben et al. (1989). For *Neogloboquadrina pachyderma* the relative abundances of right (dex.) and left (sin.) coiling individuals were determined and the two forms were treated as individual species. A detailed discussion on the planktic foraminifera fauna found in core 17748-2 is given by Marchant et al. (1999).

#### 3.3. Stratigraphic analyses

The age models for the cores 17748-2 and GeoB 3302-1 are based on accelerator mass spectrometry (AMS)  $^{14}\text{C}$  dates and stable oxygen isotope data. Both age models have been presented earlier (Lamy et al., 1999), however, here we present three additional AMS dates on core GeoB 3302-2.  $^{14}\text{C}$  AMS dates for core GeoB 3302-1 were determined on 10 mg carbonate (only shells of *Neogloboquadrina pachyderma* (dex.)) at the Leibniz Laboratory for Age Determinations and Isotope Research at the University of Kiel (Nadeau et al., 1997). Samples from core 17748-2 were analyzed at the AMS facility at the University of Groningen.

All ages are corrected for  $^{13}\text{C}$  and for a reservoir age of 400 yr (Bard, 1988) (Table 1). Although in an upwelling area as off Chile reservoir ages are most likely greater, but, since no information exists on this area, the mean ocean reservoir age of Bard (1988) has been used. The  $^{14}\text{C}$  ages were converted into calendar years using the Calib 4.0 software (Stuiver and Reimer, 1993). Ages between dated levels were obtained by linear interpolation between the nearest AMS datings. Accumulation rates are calculated according to the equations given by Van Andel et al. (1975) and by Thiede et al. (1982).

The stable oxygen isotope composition of shells of the planktic foraminifera *Neogloboquadrina pachyderma* (dex.) was measured with a Finnigan MAT 251 mass spectrometer. Twenty individual shells (>212  $\mu\text{m}$ ) were picked for each measurement. The isotopic composition of the carbonate sample was measured on the  $\text{CO}_2$  gas evolved by treatment with phosphoric acid at a constant tem-

Table 1  
AMS  $^{14}\text{C}$  dates and age control points of cores 17748-2 and GeoB 3302-1

Laboratory number <sup>a</sup>	Core depth (cm)	$^{14}\text{C}$ AMS age (yr BP)	+/- Err. (yr)	Calibrated age (cal yr BP)
Core 17748-2				
GrA 1095	69	3760	40	4230
GrA 1096	101	6890	40	7740
GrA 3805	128	9250	80	10310
GrA 1097	156	10520	50	12520
GrA 1098	185	11200	50	13060
GrA 1099	341	12890	60	15430
Core GeoB 3302-1				
	3			9790 <sup>b</sup>
KIA 4050	18	11030	160	12970
KIA 6180	33	13360	90	15940
KIA 4049	48	14950	120	17770
KIA 4044	68	15200	130	18060
KIA 4043	103	16660	150	19740
KIA 4042	133	17450	170	20640
KIA 4041	178	18590	180	21960
KIA 4040	233	19700	210	23230
KIA 6173	308	22730	240	26750
KIA 7254	405	27960	340	32700

The  $^{14}\text{C}$  ages were corrected for a reservoir effect of 400 yr (Bard, 1988) and calibrated using the Calib 4.0 software of Stuiver and Reimer (1993); for sediments older than 24000 cal yr the method of Bard (1998) has been used.

<sup>a</sup> GrA, Center for Isotope Research, University of Groningen, The Netherlands; KIA, Leibniz Laboratory, University of Kiel, Germany.

<sup>b</sup> Correlation of  $\delta^{18}\text{O}$  record to core 17748-2.

perature of 75°C. For all stable oxygen isotope measurements a working standard (Burgbrohl  $\text{CO}_2$  gas) was used, which has been calibrated against PDB by using the NBS 18, 19 and 20 standards. Consequently, all  $\delta^{18}\text{O}$  data given here are relative to the PDB standard. Analytical standard deviation is about  $\pm 0.07\%$  PDB (Isotope Lab Bremen University).

#### 4. Chronology

The stratigraphy of core 17748-2 is based on six  $^{14}\text{C}$  AMS dates and linear interpolation between the age control points (converted into calendar years, see Table 1) (Lamy et al., 1999; Marchant et al., 1999). The sediment surface with a modern age is set to -13 cm because comparison with samples of a boxcorer indicates that the uppermost 13 cm of the core is missing (Stoffers and Shipboard Scientific Party, 1992). Additionally, three turbiditic layers (9–16 cm, 47–54 cm, and

160–177 cm) are assumed to be geologically 'instantaneous' and were subtracted from the sedimentary sequence of core 17748-2. Supported by two AMS dates immediately above and below the older turbiditic layer, erosional effects can be excluded. The same is assumed for the two younger turbiditic layers. The age of the core base is approximately 15700 cal yr BP. In the Holocene section of the core sedimentation rates vary between approximately 7 and 20  $\text{cm kyr}^{-1}$ . Significantly higher sedimentation rates ( $> 70 \text{ cm kyr}^{-1}$ ) mark the oldest part of the core ( $> 13000$  cal yr BP) (Fig. 2). These are due to intensive resedimentation, probably induced by postglacial flooding of the nearby shelf (Lamy et al., 1999; Marchant et al., 1999).

The age model of core GeoB 3302-1 is also principally based on AMS dates (Table 1). Additionally, the  $\delta^{18}\text{O}$  isotope record was correlated to core 17748-2 for the uppermost sample of the core (Fig. 2). The core is estimated to cover the time span between  $\sim 9800$  and 32800 cal yr BP, which

is somewhat older than in the age model published by (Lamy et al., 1999), which was based on less AMS dates. In contrast to core 17748-2, sedimentation rates are rather low, varying between 5 and 6 cm kyr<sup>-1</sup> in the upper part of the core, representing the oldest part of the Holocene and the deglaciation. During the last glacial the sedimentation rates were high in the range of 20–40 cm kyr<sup>-1</sup> (Fig. 2).

Applying this age model, the oxygen isotope data of both cores show a typical pattern with increasing values from ~29 000 cal yr BP towards the Last Glacial Maximum (LGM) (Fig. 2). The postglacial decrease started ~18 000 cal yr BP and ended at sometime between 5000 and 8000 cal yr BP. The glacial–interglacial difference in the  $\delta^{18}\text{O}$  values is 1.9‰, which is 0.7‰ more than the global ice effect of 1.2‰ (Chappell and Shackleton, 1986). Transferred into a rough paleotemperature estimate following Epstein et al. (1953) this would indicate ~3°C colder sea surface temperatures in the study area during the LGM compared to the mid-Holocene.

## 5. Results

The bulk sedimentary data, i.e. the contents of organic carbon, carbonate and biogenic opal, display some similarities in the two cores. The CaCO<sub>3</sub> contents range between 2.1 and 17.7 wt% (Fig. 2). Between 3000 and 11 000 cal yr BP it is continuously above 12 wt%. Throughout most of the remaining time the carbonate content is <8 wt%. Comparatively low carbonate contents between 13 000 and 15 000 cal yr BP in core 17748-2 probably reflect dilution of the carbonate signal by redeposited sediments (see below). The TOC (0.27–1.44 wt%) and biogenic opal (1.1–3.1 wt%) contents show a quite similar pattern with higher values between 33 000 and 28 000 cal yr BP and during the last 10 000 yr and lower values for the intermediate period. Especially for the TOC data both records show a good agreement during the period where the two cores overlap.

The coarse fraction content (>63 µm) in both cores varies between 0 and 18 wt% (Fig. 2). How-

ever, most of the time covered it is well below 7 wt%. Only during the period 15 000–10 000 cal yr BP where the two cores overlap, coarse fraction contents >63 µm are significantly increased. In contrast, in core 17748-2 the content of the fraction >150 µm is marked by rather low values during this period.

The absolute abundance of planktic foraminifera ranges from almost 0 to ~1800 ind/gr, with almost all specimens showing a well preserved state with no indications of significant carbonate dissolution. The number of planktic foraminifera found in the older sediments of core GeoB 3302-1 is much higher (200–1200 ind/gr) than that found in the younger sediments of core 17748-2 (up to 650 ind/gr). During the overlapping period both records show quite different values, very low numbers in core 17748-2 and very high numbers in core GeoB 3302-1. The planktic foraminifera fauna in the two cores is dominated by six species (*Neogloboquadrina pachyderma* (sin.), *N. pachyderma* (dex.), *N. dutertrei*, *Globigerina bulloides*, *Globorotalia inflata* and *Globigerinita glutinata*), which account together for >90% of the total fauna. The composition of the planktic foraminifera fauna displays marked changes throughout the last 33 kyr (Fig. 3). The dominant species of the period 33 000–16 000 cal yr BP *N. pachyderma* (sin.) is gradually replaced by *N. pachyderma* (dex.) between 18 000 and 12 000 cal yr BP. The contributions of *G. glutinata* and *G. inflata* to the total fauna display quite similar patterns. During the glacial period (33 000–20 000 cal yr BP) both species have a variable relative abundance, ranging between 5% and 20%, and 5% and 30%, respectively. A period of decreasing abundances (<13% and <17%) between 20 000 and 12 500 cal yr BP is followed by rather low Holocene values of <4% for *G. glutinata* and <2% for *G. inflata*. The Holocene sediments are marked by the occurrence of *N. dutertrei*, which appeared at ~12 500 cal yr BP and which contributed between 2% and 22% to the fauna. An even higher relative abundance of up to 60% has been observed during the last 3 kyr. In contrast, comparatively little variability is displayed by *G. bulloides*. Over most of the period considered here the relative abundance of *G. bulloides* varied be-

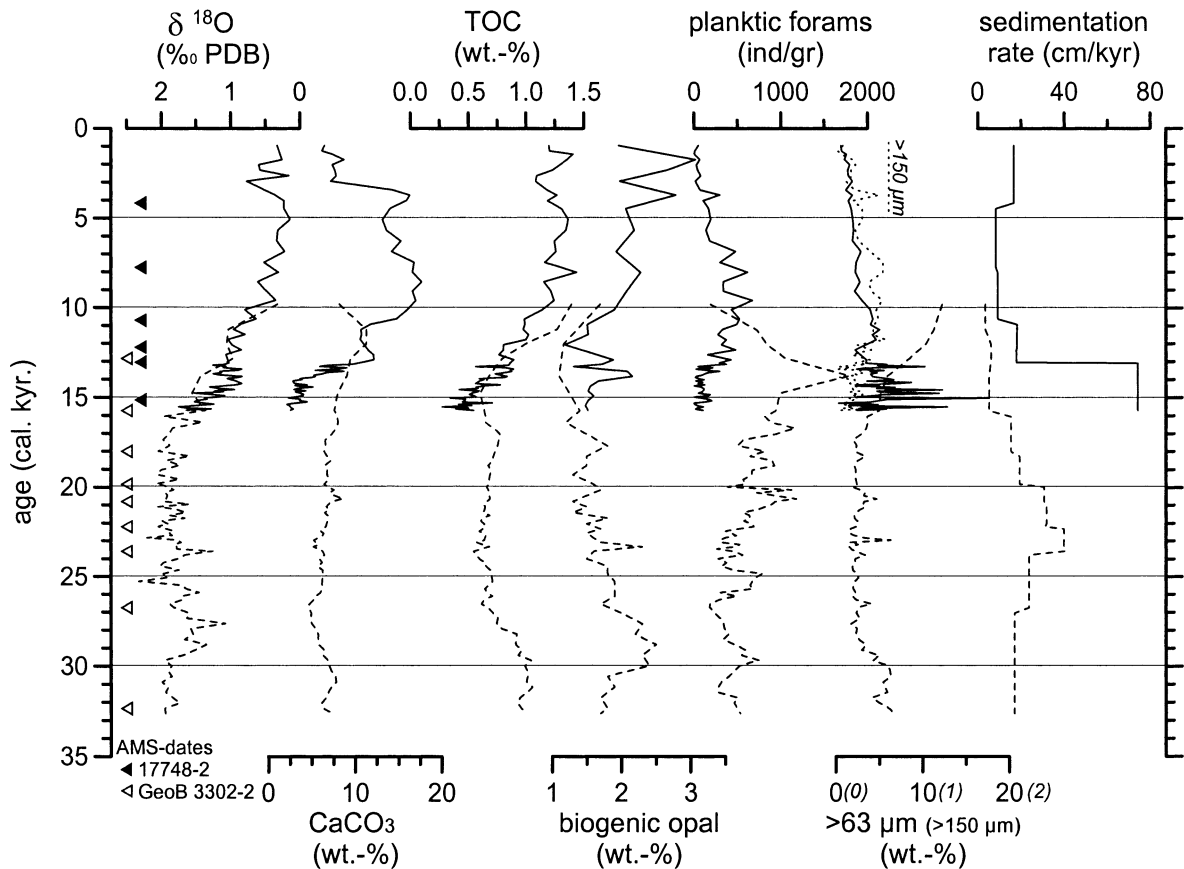


Fig. 2. Time-series records of (a) stable oxygen isotope and AMS  $^{14}\text{C}$  data, (b)  $\text{CaCO}_3$  contents, (c) TOC contents, (d) biogenic opal contents, (e) planktic foraminifera abundances, (f) grain size data and (g) sedimentation rates for cores 17748-2 (solid line) and GeoB 3302-1 (dashed line) from the Chilean continental slope.

tween 5% and 25%, with slightly lower average values between 24 000 and 29 000 cal yr BP. Only between 15 000 and 3000 cal yr BP *G. bulloides* contributes continuously between 20% and 50% to the total fauna.

## 6. Discussion

### 6.1. Reworking of sediments

As indicated by a small, but steady contribution of redeposited benthic foraminifera, some re-deposition of sediments derived from upslope seems to be a continuous process in the Valparaiso Basin (Marchant et al., 1999). Although their

absolute number keeps more or less constant throughout the core ( $< 2$  ind/gr), their relative amount is increased in the lower part of core 17748-2, probably reflecting a dilution of the accumulation of autochthonous benthic foraminifera. Based on this observation and on higher silt/clay ratios, higher silt fraction medians and, finally, extremely high sedimentation rates (Fig. 2) Marchant et al. (1999) and Lamy et al. (1999) discussed the impact of resedimentation, probably induced by the postglacial flooding of the nearby continental shelf, on the lower part of core 17748-2 corresponding to the period 15 700–13 000 cal yr BP. Strong variability in the  $> 63\text{-}\mu\text{m}$  fraction data with some very high values (Fig. 2) during this period support this conclusion.

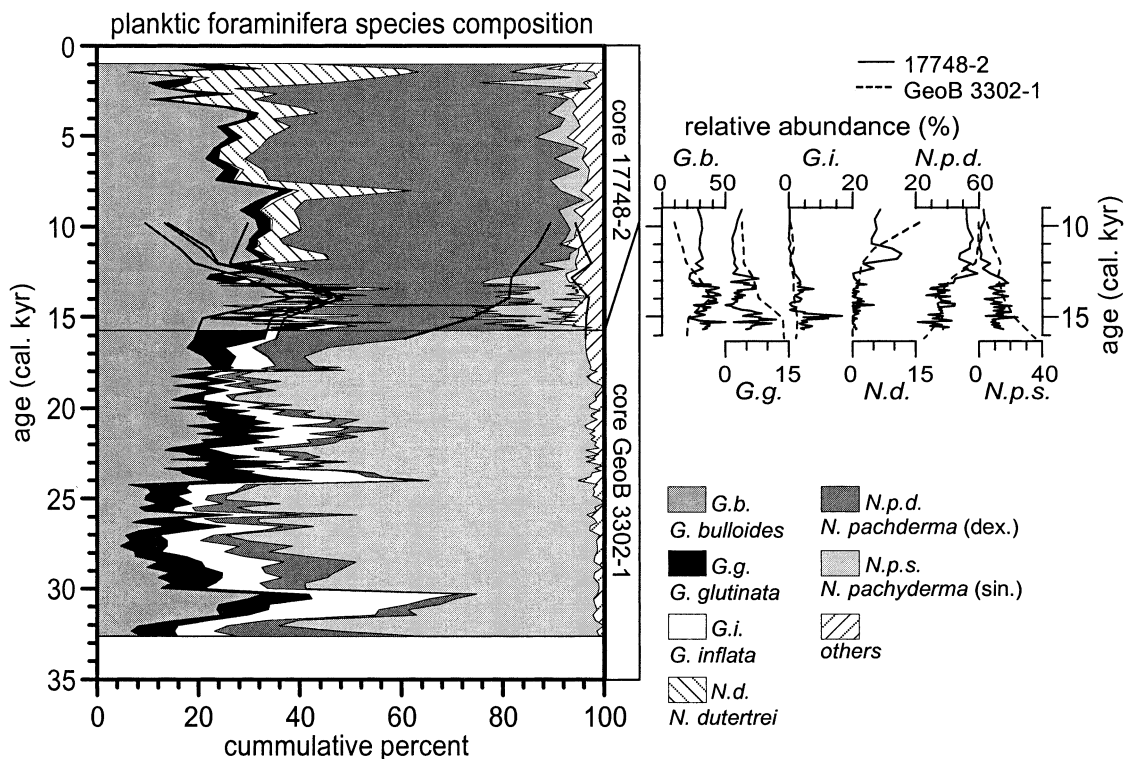


Fig. 3. Time-series record of the planktic foraminifera species composition in cores 17748-2 and GeoB 3302-1 from the Chilean continental slope. The inset shows in detail the data for individual planktic foraminifera species for the period the two cores (core 17748-2: solid line; core GeoB 3302-1: dashed line) overlap.

Also core GeoB 3302-1 seems to be affected by resedimentation, however, in a different manner. Increased coarse fraction percentages between 16000 and 10000 cal yr BP coincide with very low sedimentation rates. In spite of the fact that no sediments of the last ~10 kyr are preserved, these data indicate some winnowing at this site after 16000 cal yr BP. Thus, both cores are most likely affected by resedimentation processes such as winnowing at ~1500 m water depth (site GeoB 3302) and redeposition in ~2500 m water depth (site 17748) during the time they overlap.

However, it seems that the coarse (> 150 µm) planktic foraminifera used here (as the entire fraction > 150 µm in core 17748-2; Fig. 2) are apparently unaffected by the resedimentation processes, i.e. winnowing at site GeoB 3302 was probably not strong enough to remove such big particles,

while the energy of the resedimentation process which affected site 17748 was sufficient only to deliver mainly fine particles < 150 µm. Although the absolute abundances of planktic foraminifera in the two cores differ strongly due to dilution in core 17748 and enrichment in core GeoB 3302 (Fig. 2), the relative abundances of the various species show a high degree of similarity between the two cores (Fig. 3). As mentioned above, the planktic foraminifera species compositions in the two cores are quite different, but during the period both cores overlap (and in which resedimentation affected both cores) the relative abundances of the planktic foraminifera show the same trends in both cores, as e.g. the changing dominance between the two coiling types of *Neogloboquadrina pachyderma*, the onset of *Neogloboquadrina dutertrei* at 12500 cal yr BP, the decrease in *Globorotalia inflata* and *Globigerinita glutinata*, and the

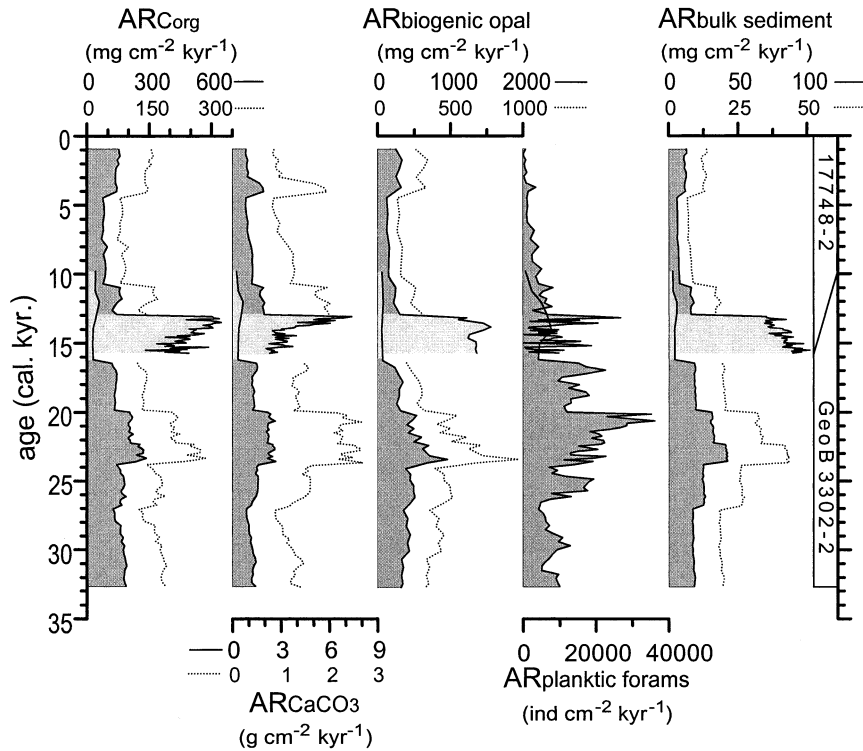


Fig. 4. Time-series records of the accumulation rates of (a) organic carbon, (b)  $\text{CaCO}_3$ , (c) biogenic opal, (d) planktic foraminifera, and (e) bulk sediment for cores 17748-2 and GeoB 3302-1 from the Chilean continental slope. The light shaded parts indicate data affected by resedimentation processes (see text). The dotted lines show the same records but refer to the expanded scales for a better demonstration of variations within the undisturbed core sections corresponding to the dark shaded parts.

relative maximum of *Globigerina bulloides* between 15 000 and 13 000 cal yr BP. The high quality of the planktic foraminifera record is further supported by the  $\delta^{18}\text{O}$  data, which during a time of distinct  $\delta^{18}\text{O}$  shifts coincide very well (Fig. 2).

Finally, also the accumulation rates of the planktic foraminifera (see below, Fig. 4) show comparable numbers during the overlapping period. This qualitative and quantitative similarity in the flux pattern of planktic foraminifera at the two sites indicates that these are almost unaffected by resedimentation, although some input of reworked planktic foraminifera at site 17748, as mentioned above for benthic foraminifera, probably occurred. However, resedimentation, in terms of near-bottom supply of sediments and winnowing, probably affected mostly finer material ( $<150\ \mu\text{m}$ ), changing both the sedimentation and bulk accumulation rates. As organic matter,

carbonate and biogenic opal are largely concentrated in the fine fraction of the sediments, these compounds are most likely affected by resedimentation. Thus, redeposition of fine material, probably derived from winnowing further upslope, increased the accumulation rates of organic matter, carbonate and biogenic opal at site 17748, while winnowing of such fine particles decreased them at site GeoB 3302, reducing the potential of these accumulation rates as paleoproductivity indicators at these sites during this period (16 000–13 000 cal yr BP). However, the planktic foraminifera accumulation rate, which is derived from the coarse fraction, seems to provide a meaningful paleoproductivity proxy also for the period between 16 000 and 13 000 cal yr BP. The other parts ( $>90\%$ ) of the entire record discussed here (33 000–16 000 cal yr BP and 13 000 cal yr BP to present) show no signs of disturbance.

## 6.2. Planktic foraminifera species composition

The most prominent change in the planktic foraminifera species composition in the study area throughout the last 33 kyr is the shift in dominance from *Neogloboquadrina pachyderma* (sin.) to *N. pachyderma* (dex.) between 18 000 and 12 000 cal yr BP (Fig. 3). Under present-day conditions the most common species along the Chilean continental slope is *N. pachyderma* (dex.), which on average accounts for > 50% in surface sediments collected between 27°S and 42°S (Hebbeln et al., 2000a). *N. pachyderma* (sin.) occurs in significant percentages only in a few samples from near-coastal sites off central Chile probably reflecting colder sea surface temperatures and/or higher productivity associated with intensive coastal upwelling (Hebbeln et al., 2000a) similar to results from the comparable Benguela Current system (Giraudeau, 1993; Little et al., 1997). At present, the two species do not show any north to south gradient in the surface sediments beneath the southern PCC, which would parallel the general sea surface temperature pattern with increasing temperatures from < 12°C in the south (45°S) to ~20°C in the north (18°S) (Hebbeln et al., 2000a).

The oxygen isotope data point to glacial surface waters ~3°C colder compared to present-day conditions, which would have resulted in similar glacial sea surface temperatures at our core sites as they are found today at ~43°S, where *Neogloboquadrina pachyderma* (dex.) still accounts for > 60% of the whole planktic foraminifera community found in surface sediments (Hebbeln et al., 2000a). Thus, the dominance of *N. pachyderma* (sin.) during the last glacial is most likely not simply due to lower temperatures induced by stronger advection of subpolar waters of the ACC, which as today were also the source waters for the PCC during the last glacial. Alternatively, the high percentages of *N. pachyderma* (sin.) prior to 18 000 cal yr BP reflect higher productivity, this interpretation being in accordance to sediment trap data from our study area (Marchant et al., 1998), indicating *N. pachyderma* (sin.) to be related to the cold, nutrient-rich coastal upwelling waters. Consequently, decreasing numbers of

*N. pachyderma* (sin.) and increasing numbers of *N. pachyderma* (dex.) indicate lower productivity during the Holocene. The significance of *N. pachyderma* (sin.) as an indicator for paleo-upwelling intensity and/or paleoproductivity has also been shown in sediments from other upwelling areas such as e.g. the Benguela Current (Little et al., 1997; Wefer et al., 1996) and the Somalia margin (Ivanova et al., 1999).

The relative changes between the *Neogloboquadrina pachyderma* species are accompanied by another significant change: the almost complete replacement of *Globorotalia inflata*, which contributed ~10% to the glacial fauna, by *Neogloboquadrina dutertrei*, which is quite common during the Holocene (Fig. 3). The similarity of the *N. pachyderma* (sin.) and *G. inflata* records is somewhat astonishing as *G. inflata* is normally not related to upwelling or high productivity. In the surface sediment data from the southern PCC *G. inflata* is more common in the open ocean samples compared to samples from the continental slope (Hebbeln et al., 2000a). However, among the slope samples those near-coastal areas marked by high abundances of *N. pachyderma* (sin.) are also marked by slightly higher percentages of *G. inflata*. Although such a pattern has not been described before, the surface sediment as well as the core data indicate that in the southern PCC higher relative abundances of *G. inflata* are related to increased coastal upwelling and/or productivity. In addition, the same general pattern with a higher relative abundance during the last glacial is also shown by the ubiquitous species *Globigerinita glutinata*.

Sediment trap investigations from the PCC indicate that *Neogloboquadrina dutertrei* is related to the Subtropical Surface Water of the PCCC (Marchant et al., 1998). Thus, the increased percentages of *N. dutertrei* during the Holocene (Fig. 3) probably reflect stronger southward advection of Subtropical Surface Water to the region (see Marchant et al., 1999, for details).

*Globigerina bulloides*, as one of the principal upwelling indicators under coastal upwelling conditions (Thiede, 1975), shows a strong seasonal association with upwelling in the modern PCC (Marchant et al., 1998). However, the core data

do not show such a distinct signal. Throughout the whole record *G. bulloides* is the second most common species, although its relative abundance shows some variability (Fig. 3). Highest percentages are found during the Holocene, when the dominance of *Neogloboquadrina pachyderma* (dex.) indicates lower productivity. During the last glacial, when higher productivity is indicated by dominating *N. pachyderma* (sin.), the relative abundance of *G. bulloides* is significantly lower. These data imply that the living conditions for *G. bulloides*, relative to those for the other species, have not changed that much, despite the drastic change indicated by the two *N. pachyderma* forms. Thus, it seems that *G. bulloides* is more related to the prevalence of upwelling rather than to its strength.

The major transition in species composition between 18 000 and 12 000 cal yr BP is marked by some internal variability (Fig. 3). The first major decline in *Neogloboquadrina pachyderma* (sin.) is partly due to a relative maximum of *Globigerinita glutinata* (16 400–14 600 cal yr BP), which includes a relative maximum of *Globorotalia inflata* (15 300–14 600 cal yr BP). The central part of the transition is marked by a maximum of *Globigerina bulloides* (14 600–13 400 cal yr BP). Before *N. pachyderma* (dex.) takes over at 13 100 cal yr BP there is another short period with elevated percentages of *G. glutinata*. This faunal sequence most likely reflects the regional shift of an upwelling cell from covering the core sites during the glacial to a more near-coastal or more southern location during the Holocene, leaving the core

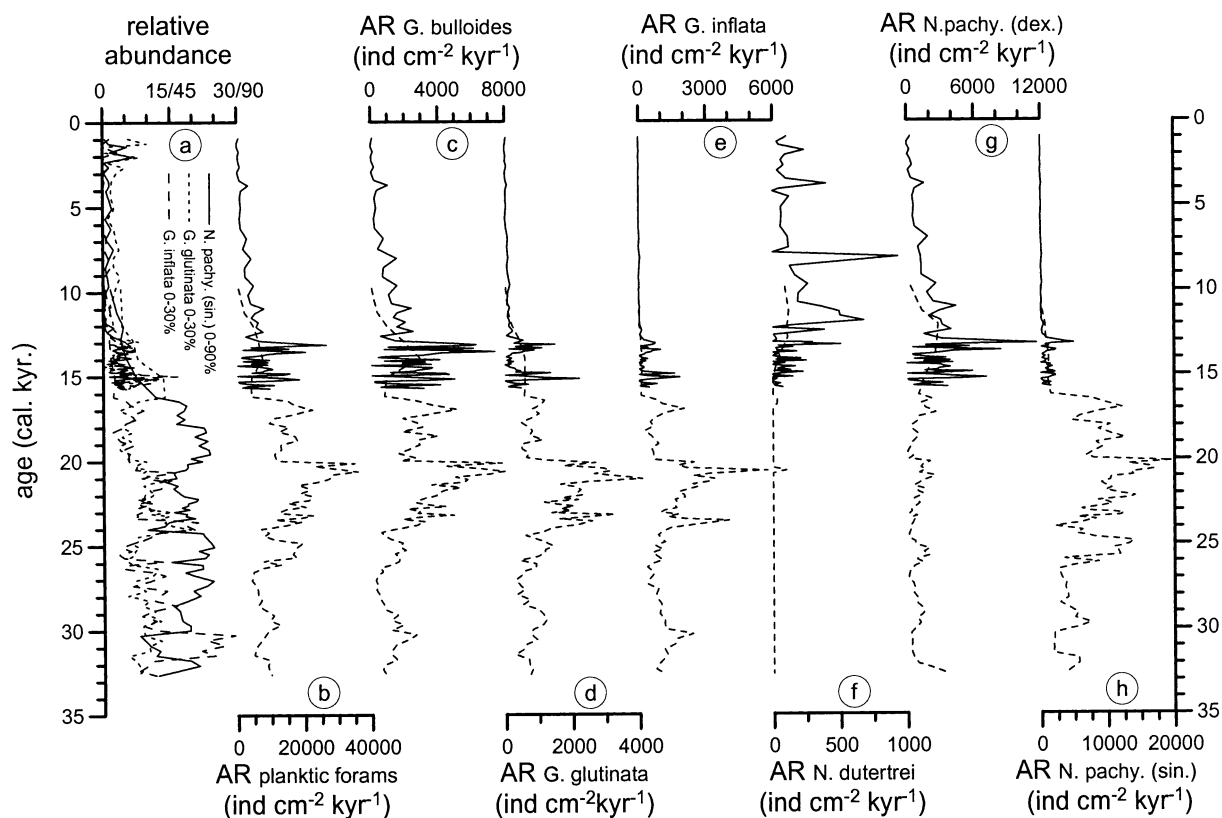


Fig. 5. Time-series records of (a) the relative abundance of the three planktic foraminifera species *Neogloboquadrina pachyderma* (sin.) (solid line), *Globigerinita glutinata* (dotted line) and *Globorotalia inflata* (dashed line) and of the accumulation rates of (b) total planktic foraminifera, (c) *Globigerina bulloides*, (d) *G. glutinata*, (e) *G. inflata*, (f) *Neogloboquadrina dutertrei*, (g) *N. pachyderma* (dex.) and (h) *N. pachyderma* (sin.) for cores 17748-2 (solid line) and GeoB 3302-1 (dashed line) from the Chilean continental slope.

sites outside the upwelling cell. The observed pattern probably marks the passage of the frontal zone bordering the upwelling waters against the open ocean waters, with *G. bulloides* having its highest relative abundance along the main front, while *G. glutinata* is more associated with the marginal frontal zone on both sides.

Also between 33 000 and 18 000 cal yr BP the species composition shows a strong variability, especially among *Neogloboquadrina pachyderma* (sin.) and *Globorotalia inflata*, but *Globigerinita glutinata* and *Globigerina bulloides* are also partly affected (Fig. 3). These species fluctuate by up to 30%, with *G. inflata*, *G. glutinata* and *G. bulloides* behaving opposite to *N. pachyderma* (sin.) (Fig. 5). As *N. pachyderma* (dex.) is almost unaffected by this variability, it is probably not caused by large scale variations in upwelling intensity, which are mainly reflected in variations among the *N. pachyderma*. However, based on the interpretation of the faunal succession found between 18 000 and 12 000 cal yr BP this variability can also be interpreted as probably caused by small variations in the extension of the upwelling cell.

Another period marked by strong variability in the species composition of the planktic foraminifera is the last 3 kyr. The unexpected pattern of simultaneously increasing relative abundances of *Neogloboquadrina duterrei*, *Neogloboquadrina pachyderma* (sin.) and *Globigerinita glutinata* (Fig. 3) has earlier been interpreted to reflect on one hand a step back to intensified upwelling and on the other hand to an increased frequency and/or intensity of El Niño events (Marchant et al., 1999). The same conclusion has been drawn from the analyses of terrigenous sediment parameters on this core, which also point to a strong climatic variability during this period (Lamy et al., 1999).

### 6.3. Paleoproductivity deduced from bulk sediment proxies

The most common tools for reconstructing paleoproductivity are the accumulation rates of biogenic compounds, as e.g. organic carbon, biogenic opal and carbonate, although subsequent processes as e.g. organic matter degradation and carbonate and opal dissolution might significantly alter

the productivity signal on its way into the sediment. However, in high productivity regions such as along the Chilean continental slope, the portion of organic carbon (Berger et al., 1989) and of biogenic opal (Nelson et al., 1995) preserved in the sediments is assumed to be significantly higher than in open ocean areas. Thus, in such a setting the accumulation rates of organic carbon and of biogenic opal should be reliable proxies for surface ocean productivity. Carbonate dissolution increases with water depth and becomes important below the lysocline, which in the study area is at ~3700 m water depth (Hebbeln et al., 2000a). The two cores studied here are from significantly lesser depths (2545 and 1498 m) and are assumed to be not seriously affected by carbonate dissolution.

The most obvious features in the accumulation rate records are the very high rates observed in the lowermost part of core 17748-2 and the extremely low rates in the uppermost part of core GeoB 3302-2 (light shaded fields in Fig. 4). As mentioned above, these extreme values are considered to be due to sediment reworking and are not relevant for estimating paleoproductivity of the PCC. The paleoproductivity of this period (16 000–13 000 cal yr BP) will be assessed by using the planktic foraminifera accumulation rate (see below).

For the remaining time of our record the accumulation rates of the bulk biogenic proxies give a detailed picture of the development of productivity off central Chile. The oldest part of the record (33 000–24 000 cal yr BP) is marked by intermediate biogenic opal ( $0.25\text{--}0.5\text{ g cm}^{-2}\text{ kyr}^{-1}$ ) and organic carbon ( $0.1\text{--}0.2\text{ g cm}^{-2}\text{ kyr}^{-1}$ ) accumulation rates associated with relatively low carbonate ( $1\text{--}2\text{ g cm}^{-2}\text{ kyr}^{-1}$ ) accumulation rates (Fig. 4). During the LGM (24 000–20 000 cal yr BP) all accumulation rates reach maximum values of  $0.5\text{--}0.9\text{ g cm}^{-2}\text{ kyr}^{-1}$  for biogenic opal,  $2\text{--}3\text{ g cm}^{-2}\text{ kyr}^{-1}$  for carbonate and  $0.2\text{--}0.3\text{ g cm}^{-2}\text{ kyr}^{-1}$  for organic carbon, respectively. This pattern clearly indicates the LGM to be the most productive period in the southern PCC throughout the last 33 kyr. Between 20 000 and 16 000 cal yr BP the accumulation rates of the biogenic compounds decrease again to intermediate levels of

0.2–0.35 g cm<sup>-2</sup> kyr<sup>-1</sup> for biogenic opal, 1.2–1.6 g cm<sup>-2</sup> kyr<sup>-1</sup> for carbonate and 0.12–0.15 g cm<sup>-2</sup> kyr<sup>-1</sup> for organic carbon, respectively, reflecting decreasing paleoproductivity.

After the break in the record the accumulation rates, now recorded in core 17748-2, remained for another 2000 yr (12 800 and 10 700 cal yr BP) on almost the same level as before the break. The following period (10 700 and 4500 cal yr BP) is characterized by the lowest biogenic accumulation rates (0.1–0.2 g cm<sup>-2</sup> kyr<sup>-1</sup> for biogenic opal, 0.7–1.3 g cm<sup>-2</sup> kyr<sup>-1</sup> for carbonate and 0.07–0.1 g cm<sup>-2</sup> kyr<sup>-1</sup> for organic carbon) of the whole record. During this period the distance between the core sites and any nearby upwelling center was probably the largest throughout the last 33 kyr resulting in a relatively low paleoproductivity. The youngest part of the record (<4500 cal yr BP) is again marked by slightly higher accumulation rates, which are in a similar range as between 12 800 and 10 700 cal yr BP, with the exception of the carbonate accumulation rate, which drops back to lowest values after 3000 cal yr BP. However, in general the Late Holocene is marked by a higher paleoproductivity than the Early and Middle Holocene.

#### 6.4. Paleoproductivity deduced from planktic foraminifera accumulation rates

The accumulation rates of the most common species of planktic foraminifera off central Chile show two dominant patterns (Fig. 5). *Neogloboquadrina pachyderma* (sin.), *Globorotalia inflata* and *Globigerinita glutinata* are characterized by high accumulation rates during the last glacial and extremely low rates during the Holocene (Fig. 5d,e,h). The accumulation rates of the latter two species have a clearly defined maximum between 24 000 and 20 000 cal yr BP (Fig. 5d,e), while the maximum for the former species lasted from 26 000 to 16 000 cal yr BP (Fig. 5h). During the remaining periods between 33 000 and 16 000 cal yr BP the accumulation rates of these three species are still on relatively high levels.

In contrast, *Neogloboquadrina pachyderma* (dex.) and *Neogloboquadrina dutertrei* have their highest fluxes between 16 000 and 9000 cal yr BP

and between 12 000 and 8000 cal yr BP, respectively (Fig. 5f,g). While the *N. pachyderma* (dex.) flux steadily decreases after 9000 cal yr BP towards the present, the *N. dutertrei* flux fluctuates around a stable mean ( $\sim 100$  ind cm<sup>-2</sup> kyr<sup>-1</sup>) during the last 8 kyr. During the last glacial the accumulation rates of *N. pachyderma* (dex.) were relatively low, while *N. dutertrei* was completely absent.

The accumulation rate of *Globigerina bulloides* displays an intermediate pattern (Fig. 5c). During the last glacial it follows closely the pattern of *Globigerinita glutinata* and *Globorotalia inflata*, while during the younger part of the record it almost resembles the accumulation rate pattern of *Neogloboquadrina pachyderma* (dex.). Interestingly, the accumulation rates of all planktic foraminifera show an almost identical pattern as the accumulation rate of *G. bulloides* (Fig. 5b,c), which over the whole record accounts only for 23% of the total fauna.

These data reflect the different response of the various species to changing environmental conditions in the southern PCC. The accumulation rate of all planktic foraminifera probably reflects the general pattern of paleoproductivity with significantly higher values during the glacial compared to the Holocene, as it can also be seen in the accumulation rates of the other biogenic compounds (Fig. 4). Obviously, *Neogloboquadrina pachyderma* (sin.), *Globigerinita glutinata*, *Globorotalia inflata*, and *Globigerina bulloides* find best living conditions during periods of high productivity, resulting in the highest flux rates of these species. Under such conditions the competition among the species seems to be too strong for *N. pachyderma* (dex.) to sustain a larger population. However, decreasing productivity after 16 000 cal yr BP resulted in more favorable environmental conditions for *N. pachyderma* (dex.) and since 12 000 cal yr BP also *Neogloboquadrina dutertrei* found suitable conditions. Although *G. bulloides* has its highest relative abundance during the Middle Holocene (Fig. 3), accumulation rates are much lower than during the last glacial, reflecting in general worse conditions for *G. bulloides* during the Holocene.

As mentioned above, the total planktic forami-

nifera accumulation rate shows almost the same pattern as the accumulation rates for the other biogenic compounds (Fig. 4). However, comparing it especially with the carbonate accumulation rate displays some differences during the Holocene, when the total planktic foraminifera accumulation rate continuously decreases, while the carbonate accumulation rate is much more stable (Fig. 4). This difference becomes even more obvious when comparing the contents of planktic foraminifera and carbonate for the investigated cores (Fig. 6). There are three distinct relations between these two data sets in the two cores. One, marked by the steepest slope, is valid for core GeoB 3302-2 and, thus, for the last glacial (32 600–15 000 cal yr BP). The steep slope implies that the contribution of planktic foraminifera to the carbonate content is relatively high. In contrast, the slopes for the two other relations, both

are valid for core 17748-2, are much shallower, implying a larger contribution of other carbonate particles. Since benthic foraminifera contribute mostly < 5% to the whole foraminifera assemblage, except of those core sections where total foraminifera numbers and carbonate contents are very low (at the top and base of core 17748 and at the top of GeoB 3302), the most likely candidates to contribute significantly to the carbonate content are coccoliths, which seem to become increasingly important in the period 15 700–9000 cal yr BP, and even more in the period marked by the shallowest slope (the last 9 kyr).

The higher contribution of coccoliths to site 17748-2 might reflect a different setting at this site compared to site GeoB 3302-2. However, the data for the oldest part (15 700–14 200 cal yr BP, hatched field in Fig. 6), which fit nice into the relation covering the whole period up to 9000 cal

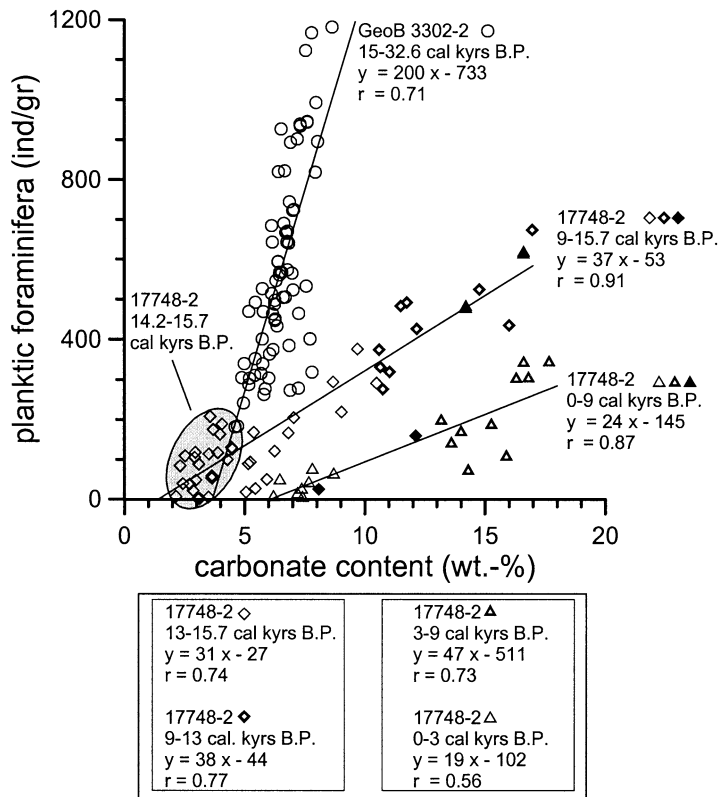


Fig. 6. Absolute abundance of planktic foraminifera versus CaCO<sub>3</sub> content in cores 17748-2 and GeoB 3302-1 from the Chilean continental slope. The various regression lines reflect different levels of planktic foraminifera contribution to the total CaCO<sub>3</sub> content at different times (see text).

yr BP, fit also perfectly to the data of core GeoB 3302-2, indicating a general shift in the environmental setting between 15 700 and ~14 000 cal yr BP, affecting both sites. The increasing importance of coccoliths from glacial to Holocene times is another indicator for a parallel decrease in productivity, as coccoliths are the typical primary producers in less productive waters, compared to diatoms, which are typical for high productivity conditions.

#### 6.5. Factors controlling the paleoproductivity off central Chile during the last 33 kyr

Comparing the normalized accumulation rates of organic carbon, carbonate and biogenic opal for the undisturbed sedimentary records (dark hatched periods in Fig. 4) results in a quite coherent picture (Fig. 7). These data fit to the normalized accumulation rate of planktic foraminifera, which, in addition, provide a meaningful indication for the paleoproductivity between 16 000 and 13 000 cal yr BP (Fig. 7). The normalized accumulation rates of organic carbon, carbonate and biogenic opal have been combined to the paleoproductivity index (bold line in Fig. 7a) introduced here, which simply is the mean of these normalized accumulation rates. The paleoproductivity index gives a robust qualitative estimate of the development of the paleoproductivity in the southern PCC, which is independently supported by the species composition data of the planktic foraminifera (Fig. 3).

According to these data the paleoproductivity in the southern PCC has been developed rather variable through the last 33 kyr. Between 33 000 and 24 000 cal yr BP it remained on an intermediate level followed during the LGM by the highest paleoproductivity (Fig. 7). After 20 000 cal yr BP the paleoproductivity dropped rapidly to the pre-LGM level and decreased further to minimum values between 8 000 and 4 000 cal yr BP. This decrease is characterized by some internal fluctuations, namely a slight increase in productivity between 13 000 and 11 000 cal yr BP. During the last 4 kyr the paleoproductivity returned to an intermediate level, similar to pre-LGM times (Fig. 7).

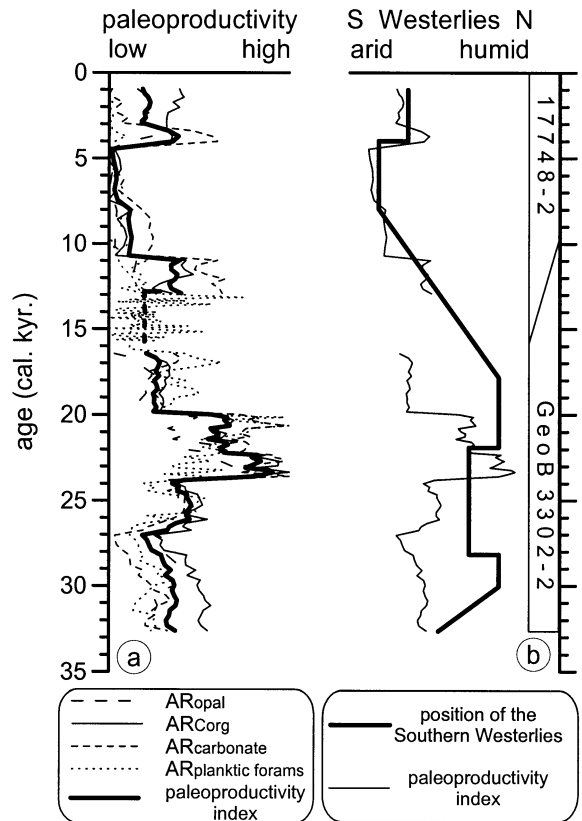


Fig. 7. (a) Comparison of the normalized accumulation rates of organic carbon,  $\text{CaCO}_3$ , biogenic opal and planktic foraminifera combined to the paleoproductivity index, which is the mean of the normalized accumulation rates of organic carbon,  $\text{CaCO}_3$  and biogenic opal. The data have been normalized to a 0–1 scale (1) by subtracting the minimum value from all data within one data set and (2) by dividing them through the maximum minus minimum value. (b) Comparison of the paleoproductivity index with the relative latitudinal position of the Southern Westerlies taken from Lamy et al. (1999).

Pollen (Heusser, 1989) and marine sedimentological (Lamy et al., 1998, 1999) studies suggest an approximately  $5^\circ$  northward displacement of the climatic zones in Chile during the LGM induced by a northward shift of the Southern Westerlies. We assume that such a change would also shift the whole oceanographic system along the Chilean continental slope towards the north. Based on a continental paleoclimate reconstruction on the base of the same sediment cores used here, Lamy et al. (1999) described the vari-

ability of the position of the Southern Westerlies, which controls the regional climate (Miller, 1976), through the last 33 kyr. Interestingly, the pattern of latitudinal movements of the Southern Westerlies shows similarity to the paleoproductivity pattern, i.e. higher productivity is related to a northern position and lower productivity to a southern position of the Southern Westerlies (Fig. 7). Besides being similar in the long run, both records also agree in small scale structures, as e.g. the shift to higher productivity coinciding with a northward movement of the Southern Westerlies at 4000 cal yr BP.

The similarity of these two records points to a functional relationship between the position of the Southern Westerlies and the productivity in the study region. A hint as to how this relationship could look like has been found in the surface sediments of the Chilean continental slope (Hebbeln et al., 2000a). Gradually decreasing organic carbon accumulation rates, in accordance with decreasing satellite-derived pigment concentrations (Thomas et al., 1994), and increasing  $\delta^{15}\text{N}$  data from south to north along the Chilean continental slope point to the high-nutrient and low-chlorophyll waters of the ACC as the principal nutrient source sustaining the high productivity in the coastal upwelling system of the southern PCC supplemented by micronutrients (e.g. iron) derived from nearby hinterland (Hebbeln et al., 2000a). Latitudinal movements of the Southern Westerlies are almost certainly directly related to variations in the northward extension of the ACC. Thus, a northward position of the Southern Westerlies coincides with a northward expansion of the ACC, which in turn brings our core sites closer to the main nutrient source which, analogous to the surface sediment data, would result in increased nutrient availability and consequently in increased productivity at these sites.

In addition to this variable nutrient supply to our study area, also the intensity of coastal upwelling, as interpreted from the varying species composition of the planktic foraminifera, has probably changed, what might be due to a variable wind forcing in line with the latitudinal movements of the main climatic zonation in the region. The coastal upwelling is an extremely im-

portant part of the whole production system, acting like a vortex-type conveyor belt transporting nutrient-rich waters derived from the ACC northwards. By returning nutrients to the productive zone, upwelling keeps the (pre-formed) nutrients supplied by the ACC and transported northward by the PCC within the productive system. Thus, the effect of upwelling on productivity off Chile is strongly related to the amount of (pre-formed) nutrients in the system, which mainly depends on the distance of a given site to the main nutrient source.

Both the paleoproductivity off Chile and the continental paleoclimate in Chile seem to be mainly driven by the setting of the large scale climatic zonation in the Southeast Pacific region. To what extent small scale variations in the position of the Southern Westerlies on Dansgaard/Oeschger time scales, which have been detected in older sediments (60 000–25 000 cal yr BP) off northern Chile (Lamy et al., 2000) and which might be reflected in the variability in the faunal composition of the planktic foraminifera in the oldest part of the record presented here, did affect the paleoproductivity pattern off Chile needs to be determined in future studies.

## 7. Conclusions

The data presented here clearly indicate a significantly higher productivity in the southern PCC during the LGM compared to the Holocene. However, based on the unequivocal data from the Antarctic region (Keir, 1990; Mackensen et al., 1994; Mortlock et al., 1991) and based on our understanding of the functioning of the upwelling/productivity system in the southern PCC (Hebbeln et al., 2000a), we do not draw this conclusion at the moment. The data might reflect only a northward shift of the main upwelling area in pace with the latitudinal shifts of the Southern Westerlies, resulting for the LGM on one hand in a higher productivity but on the other hand in a lower productivity further to the south. This interpretation has also been discussed for the subantarctic region (Mackensen et al., 1994), which for both regions would be basically

due to the same reason: a northward displacement of the circum-Antarctic circulation. Thus, to finally assess the productivity of the southern PCC on glacial–interglacial time scales further reconstructions of the paleoproductivity from this region covering a larger latitudinal range are needed.

### Acknowledgements

We thank M. Segl and B. Meyer-Schack, who performed the stable isotope measurements, and B. Bohling, who run the opal analyses. We are also indebted to W.H. Berger, F. Lamy and R. Schneider for helpful comments on an earlier version of the manuscript. This study was supported by the German Bundesministerium für Bildung und Forschung through funding of the project ‘CHIPAL’ (SO-102). M.M. acknowledges financial support by the Deutscher Akademischer Austauschdienst (DAAD).

### References

- Alheit, J., Bernal, P., 1993. Effects of physical and biological changes on the biomass yield of the Humboldt Current ecosystem. In: Sherman, K., Alexander, L.M., Gold, B.D. (Eds.), Large Marine Ecosystems. V: Stress, Mitigation and Sustainability. American Association for the Advancement of Science, Washington, DC, pp. 55–68.
- Bard, E., 1988. Correction of accelerator mass spectrometry  $^{14}\text{C}$  ages measured in planctonic foraminifera: Paleoceanographic implications. *Paleoceanography* 3, 635–645.
- Bard, E., 1998. Geochemical and geophysical implications of the radiocarbon calibration. *Geochim. Cosmochim. Acta* 62, 2025–2038.
- Barnola, J.M., Raynaud, D., Korotkevich, Y.S., Lorius, C., 1987. Vostok ice core provides 160000-year record of atmospheric  $\text{CO}_2$ . *Nature* 329, 408–414.
- Berger, W.H., Herguera, J.C., 1992. Reading the sedimentary record of the ocean’s productivity. In: Falkowski, P.F., Woodhead, A.D. (Eds.), Primary Productivity and Biogeochemical Cycles in the Sea. Plenum Press, New York, pp. 455–486.
- Berger, W.H., Fischer, K., Lai, C., Wu, G., 1987. Ocean productivity and organic carbon flux. Part I. Overview and maps of primary production and export production. *SIO Ref.* 87-30.
- Berger, W.H., Smetacek, V.S., Wefer, G., 1989. Ocean productivity and paleoproductivity – an overview. In: Berger, W.H., Smetacek, V.S., Wefer, G. (Eds.), Productivity of the Ocean: Present and Past. Wiley, New York, pp. 1–34.
- Boltovskoy, E., 1976. Distribution of recent foraminifera of the South America region. In: Hedley, R.H., Adams, C.G. (Eds.), Foraminifera. Academy Press, New York, pp. 171–236.
- Brandhorst, W., 1963. Descripción de las condiciones oceanográficas en las aguas costeras entre Valparaíso y el golfo de Arauco, con el especial referencia al contenido de oxígeno y su relación con la pesca (resultados de la expedición AGRIMAR). Dirección de Agricultura y Pesca, Ministerio de Agricultura, Santiago de Chile, 55 pp.
- Broecker, W.S., 1982. Ocean chemistry during glacial time. *Geochim. Cosmochim. Acta* 46, 1689–1705.
- Chappell, J., Shackleton, N.J., 1986. Oxygen isotopes and sea level. *Nature* 324, 137–140.
- DeMaster, D.J., 1981. The supply and accumulation of silica in the marine environment. *Geochim. Cosmochim. Acta* 45, 1715–1732.
- Epstein, S., Buchsbaum, R., Lowenstamm, H.A., Urey, H.C., 1953. Revised carbonate-water isotopic temperature scale. *Bull. Geol. Soc. Am.* 64, 1315–1325.
- Giraudeau, J., 1993. Planktonic foraminiferal assemblages in surface sediments from the southwest African continental margin. *Mar. Geol.* 110, 1–16.
- Hebbeln, D., Marchant, M., Freudenthal, T., Wefer, G., 2000a. Surface sediment distribution along the Chilean continental slope related to upwelling and productivity. *Mar. Geol.* 164, 119–137.
- Hebbeln, D., Marchant, M., Wefer, G., 2000b. Seasonal variations of the particle flux in the Peru–Chile Current at 30°S under ‘normal’ and under El Niño conditions. *Deep-Sea Res. II* 47, 2101–2128.
- Hebbeln, D., Wefer, G., Cruise Participants, 1995. Cruise Report of R/V *Sonne* Cruise 102, Valparaíso–Valparaíso, 9.5.95–28.6.95. *Ber. Fachbereich Geowiss.* 68. Universität Bremen, Bremen, 126 pp.
- Hemleben, C., Spindler, M., Anderson, O.R., 1989. Modern Planktonic Foraminifera. Springer, New York, 335 pp.
- Heusser, C.J., 1989. Southern westerlies during the Last Glacial Maximum. *Quat. Res.* 31, 423–425.
- Ivanova, E.M., Conan, S.M.H., Peeters, F.J.C., Troelstra, S.R., 1999. Living *Neogloboquadrina pachyderma* sin and its distribution in the sediments from Oman and Somalia upwelling areas. *Mar. Micropaleontol.* 36, 91–107.
- Keir, R.S., 1990. Reconstructing the ocean carbon system variation during the last 150–000 years according to the Antarctic nutrient hypothesis. *Paleoceanography* 5, 253–276.
- Kennett, J.P., Srinivasan, M., 1983. Neogene Planktonic Foraminifera. Hutchinson Ross, Stroudsburg, PA, 265 pp.
- Lamy, F., Hebbeln, D., Wefer, G., 1998. Late Quaternary precessional cycles of terrigenous sediment input off the Norte Chico, Chile (27.5°S) and paleoclimatic implications. *Palaeogeogr. Palaeoclimatol. Palaeoecol.* 141, 233–251.
- Lamy, F., Hebbeln, D., Wefer, G., 1999. High resolution marine record of climatic change in mid-latitude Chile during

- the last 28 ka based on terrigenous sediment parameters. *Quat. Res.* 51, 83–93.
- Lamy, F., Klump, J., Hebbeln, D., Wefer, G., 2000. Late Quaternary rapid climate change in northern Chile. *Terra Nova* 12, 8–13.
- Little, M.G., Schneider, R., Kroon, D., Price, B., Summerhayes, C.P., Segl, M., 1997. Trade wind forcing of upwelling, seasonality, and Heinrich events as a response to sub-Milankovitch climate variability. *Paleoceanography* 12, 568–577.
- Lyle, M., 1988. Climatically forced organic carbon burial in equatorial Atlantic and Pacific Oceans. *Nature* 335, 529–532.
- Mackensen, A., Grobe, H., Hubberten, H.W., Kuhn, G., 1994. Benthic foraminiferal assemblages and the  $\delta^{13}\text{C}$ -signal in the Atlantic sector of the Southern Ocean: glacial-to-interglacial contrasts. In: Zahn, R., Pedersen, T.F., Kaminski, M., Labeyrie, L. (Eds.), *Carbon Cycling in the Glacial Ocean: Constraints on the Ocean's Role in Global Change*. Springer, Berlin, pp. 105–144.
- Marchant, M., Hebbeln, D., Wefer, G., 1998. Seasonal flux patterns of planktic foraminifera in the Peru–Chile Current. *Deep-Sea Res.* 45, 1161–1185.
- Marchant, M., Hebbeln, D., Wefer, G., 1999. High resolution planktic foraminiferal record of the last 13–000 years from the upwelling area off Chile. *Mar. Geol.* 161, 115–128.
- McIntyre, A., Ruddiman, W.F., Karlin, K., Mix, A.C., 1989. Surface water response of the equatorial Atlantic Ocean to orbital forcing. *Paleoceanography* 4, 19–55.
- Miller, A., 1976. The climate of Chile. In: *Schwerdtfeger, W.* (Ed.), *World Survey of Climatology*, Vol. 12. Elsevier, Amsterdam, pp. 113–145.
- Mortlock, R.A., Charles, C.D., Froelich, P.N., Zibello, M.A., Saltzman, J., Hays, J.D., Burckle, L.H., 1991. Evidence for lower productivity in the Antarctic Ocean during the last glaciation. *Nature* 351, 220–223.
- Müller, P.J., Schneider, R., 1993. An automated leaching method for the determination of opal in sediments and particulate matter. *Deep-Sea Res.* 40, 425–444.
- Nadeau, M.J., Schleicher, M., Grootes, P.M., Erlenkeuser, H., Gottolung, A., Mous, D.J.W., Sarnthein, J.M., Willkomm, N., 1997. The Leibniz-Labor AMS Facility at the Christian-Albrechts University, Kiel, Germany. *Nucl. Instrum. Methods Phys. Res.* 123, 22–30.
- Nelson, D.M., Tréguer, P., Brzezinski, M.A., Leynaert, A., Quéguiner, B., 1995. Production and dissolution of biogenic silica in the ocean: Revised global estimates, comparison with regional data and relationship to biogenic sedimentation. *Glob. Biogeochem. Cycles* 9, 359–372.
- Parker, F.L., 1962. Planktonic foraminiferal species in Pacific sediments. *Micropaleontology* 8, 219–254.
- Rühlemann, C., Müller, P.J., Schneider, R.R., 1999. Organic carbon and carbonate as paleoproductivity proxies: Examples from high and low productivity areas of the tropical Atlantic. In: Fischer, G., Wefer, G. (Eds.), *Use of Proxies in Paleoceanography*. Springer, Berlin, pp. 315–344.
- Sarnthein, M., Winn, K., 1990. Reconstruction of low and middle latitude export productivity, 30 000 years to present: Implications for global carbon reservoirs. In: Schlesinger, M. (Ed.), *Climate–Ocean Interaction*. Kluwer Academic Publishers, Dordrecht, pp. 319–342.
- Schneider, R.R., Müller, P.J., Ruhland, G., Meinecke, G., Schmidt, H., Wefer, G., 1996. Late Quaternary surface temperatures and productivity in the East-Equatorial South Atlantic: Response to changes in trade/monsoon wind forcing and surface water advection. In: Wefer, G., Berger, W.H., Siedler, G., Webb, D.J. (Eds.), *The South Atlantic: Present and Past Circulation*. Springer, Berlin, pp. 527–551.
- Shaffer, G., Salinas, S., Pizarro, O., Vega, A., Hormazabal, S., 1995. Currents in the deep ocean off Chile (30°S). *Deep-Sea Res.* 42, 425–436.
- Stoffers, P., Shipboard Scientific Party, 1992. Cruise report *Sonne 80a – Midplate III oceanic volcanism in the Southeast Pacific*. *Berichte. Universität Kiel*, Kiel, 128 pp.
- Strub, P.T., Mesias, J.M., Montecino, V., Rutlant, J., Salinas, S., 1998. Coastal ocean circulation off Western South America. In: Robinson, A.R., Brink, K.H. (Eds.), *The Global Coastal Ocean. The Sea*. Wiley, New York, pp. 273–314.
- Stuiver, M., Reimer, P.J., 1993. Extended  $^{14}\text{C}$  data-base and revised calib. 3.0 C-14 age calibration program. *Radiocarbon* 35, 215–230.
- Thiede, J., 1975. Distribution of foraminifera in surface waters of a coastal upwelling area. *Nature* 253, 712–714.
- Thiede, J., Suess, E., Müller, P.J., 1982. Late Quaternary fluxes of major sediment component to the sea floor at the Northwest African continental slope. In: von Rad, U., et al. (Eds.), *Geology of the Northwest African Continental Margin*. Springer, New York, pp. 605–631.
- Thomas, A.C., Huang, F., Strub, P.T., James, C., 1994. Comparison of the seasonal and interannual variability of phytoplankton pigment concentrations in the Peru and California Current systems. *J. Geophys. Res.* 99 (C4), 7355–7370.
- Van Andel, T.H., Heath, T.H., Moore, T.C., 1975. Cenozoic history and paleoceanography of the central Pacific Ocean. *Mem. Geol. Soc. Am.* 143, 134 pp.
- Wefer, G. et al., 1996. Late Quaternary surface circulation of the South Atlantic: The stable isotope record and implications for heat transport and productivity. In: Wefer, G., Berger, W.H., Siedler, G., Webb, D.J. (Eds.), *The South Atlantic: Present and Past Circulation*. Springer, Berlin, pp. 461–502.